

Inconel 713 and TiAl turbine blade impact test validation with LS-Dyna, including Inconel 718 casing and failure models

Kevin Manzanera¹, [Izei Catalina](#)¹

¹ITP Aero, Industria de Turbo Propulsores, S.A.U. Zamudio – Spain

1 Abstract

Motivated by the necessity of validating new materials for future turbines, a set of Blade Crush Tests have been performed with Inconel 713 blades, TiAl blades, Inconel 718 casing material and steel plates. The objective of these tests is to study separately the deformation of a blade during a containment event (configuration 1 tests), and the damage of the casing caused by the impact of different blades (configuration 2 tests). The results of these tests are validated with LS-Dyna analysis, providing a reliable tool for predicting the containment capability of the casings and the out of balance progression in a blade off event. This will allow to assess the containment capability of future designs without the need of large and very costly test campaigns or service experience.

The results and analysis validation obtained from configuration 1 tests are representative of the initial impact sequence of a containment event with Inconel 713 and TiAl blades. Inconel 713 blades will bend after tip contact with the casing and the shroud is likely to break. TiAl blade will shatter after tip contact with the casing and cracks will propagate through the aerofoil. Configuration 2 does not fully represent the damage and impact sequence expected in a containment event. The damage observed in these tests is likely to be higher than the expected on a containment event. Cracks observed in the plates correlate well with the analyses. This suggests that a containment analysis would also correlate well with a real containment event, even though the impact sequence is slightly different.

The work presented in this paper shows the capability of ITP Aero to perform impact rig tests that represent the initial containment impact conditions. This will allow to test and compare the impact behaviour of different blade and casing materials in containment like conditions.

2 Introduction

The constant development on gas turbine engines will require that future turbines work in more demanding conditions, such as, higher rotational speeds and higher temperatures. This has lead up to the development of new materials for the turbine casing and blades. In this scenario, it is necessary to understand the behaviour of these new materials in impact conditions and develop specific methods that are applicable to these new designs.

According to the civil aerospace regulatory requirements [1], *“It must be demonstrated that any single compressor or turbine blade will be contained after Failure”*. This is called the containment capability of the casing. It is also required that *“no Hazardous Engine Effect can arise as a result of other Engine damage likely to occur before Engine shut down following a blade Failure”*. Note that the consequences after a blade failure may be guided by the out of balance (OoB) generated in the event. Considering these two requirements, it is necessary to understand both the impact absorption capability of the casing and the interaction between the release blade and the rotor.

A strategy that involves specific rig tests and validation with analysis has been approached. As the beginning of this strategy, a set of Blade Crush Tests have been performed with Inconel 713 blades, TiAl blades, Inconel 718 casing material and steel plates. The objectives of these tests is to study separately the deformation of a blade during a containment event (configuration 1 tests), and the damage of the casing caused by different blades (configuration 2 tests). The results of these tests are validated with LS-Dyna analysis, providing a reliable tool for predicting the containment capability of the casings and the out of balance (OoB) progression in a blade off event.

The work of other authors has been focused on validating casing material properties with multiaxial and ballistic testing [2], [3], [4] where the deformation of the projectile is not so relevant. The work presented in this paper is a further step in the validation of containment events with LS-Dyna, which includes the validation of the impact sequence, the deformation of the projectile (blade) and the deformation of the casing.

3 Nomenclature

OoB	Out of Balance
HSC	High Speed Camera
SG	Strain Gauge
DIC	Digital Image Correlation
HS	High Speed
LS	Low Speed

4 Test description

Two configurations were tested in order to study separately the deformation of a blade during a containment event (configuration 1), and the damage of the casing caused by different blades (configuration 2). High speed cameras and strain-gauges were used in order to measure the blade behaviour and the impact impulse in the specimens. All the tests were carried out at room temperature and in vacuum conditions.

Configuration 1 tests consisted in shooting flat rigid plates (blue) to blade tips in order to represent the damage of the blade when hitting the casing. Blades were located with no movement restriction in order to represent free conditions of a blade-off event. See Figure 1:

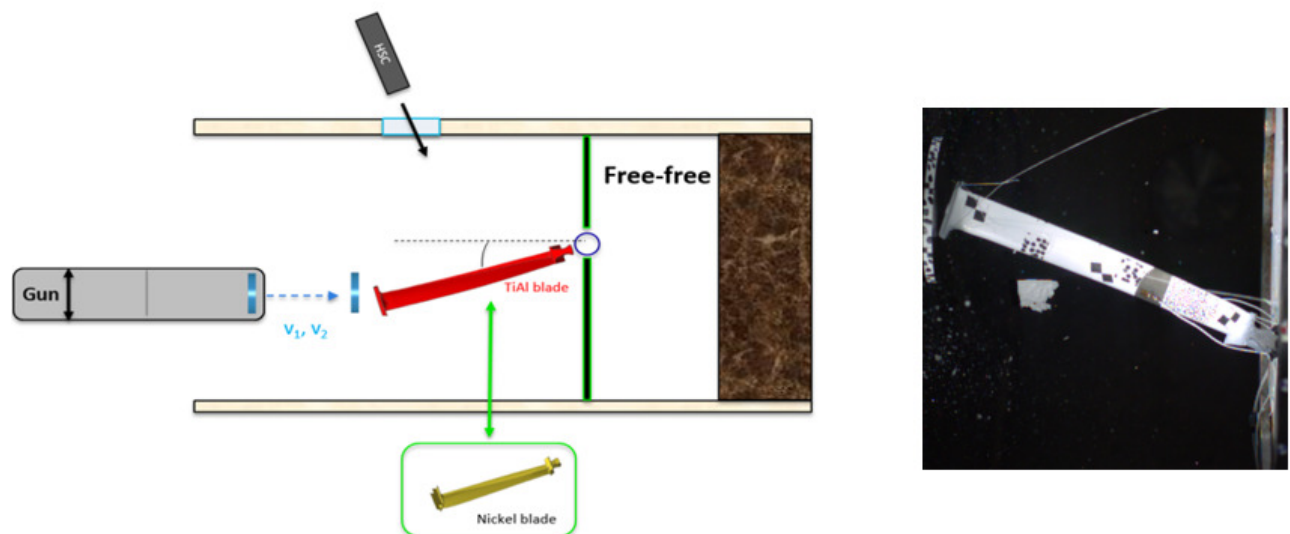


Fig.1: Blade Crush Test. Configuration 1 test scheme (left) and rig set up (right). Flat rigid projectiles (blue), TiAl blade (red), Inconel 713 blade (yellow).

Configuration 2 tests consisted in shooting blades to deformable plates in order to compare the damage caused by different blades. See Figure 2:

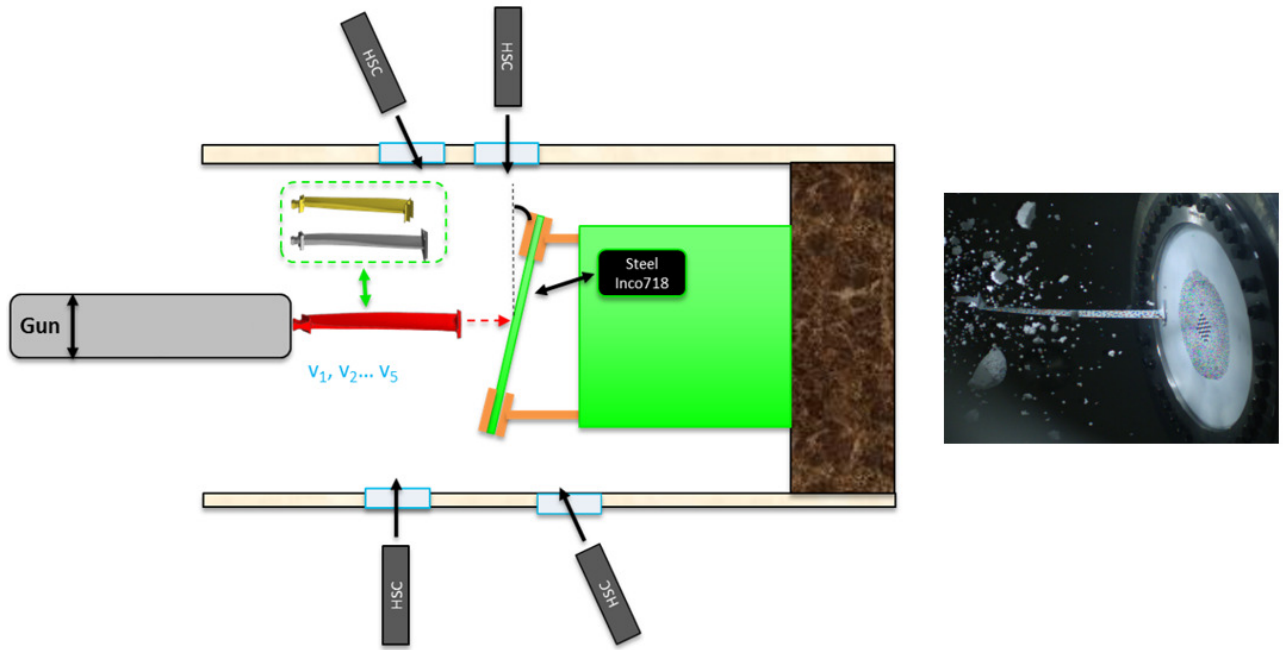


Fig.2: Blade Crush Test. Configuration 2 test scheme (left) and rig set up (right). Steel/Inconel 718 plates (green), TiAl blade (red), Inconel 713 blades (yellow and grey).

Sensitivity to blade material, blade shape, impact speed and casing material was studied. These parameters were selected in order to represent different engine conditions and obtain conclusions applicable to different engines.

The following test matrix was performed (see Table 1 and Table 2):

Configuration 1				
#	Blade Mat	Casing Material	Speed (m/s)	Comments
1	Inconel 713	Steel	HS	Repeatability
2	Inconel 713	Steel	HS	
3	Inconel 713	Steel	HS	
4	Inconel 713	Steel	HS	
5	Inconel 713	Steel	LS	Speed sensitivity
6	Inconel 713	Steel	LS	
7	TiAl	Steel	HS	Blade material sensitivity
8	TiAl	Steel	HS	
9	TiAl	Steel	HS	
10	FAIL			
11	TiAl	Steel	LS	Speed sensitivity
12	TiAl	Steel	LS	

Table 1: Blade Crush Test Matrix, Configuration 1. HS (high speed) and LS (low speed) impacts

Configuration 2				
#	Blade Mat	Plate Material	Speed (m/s)	Comments
13	Inconel 713	Steel	HS	Speed sensitivity
14	Inconel 713	Steel	HS	
15	Inconel 713	Steel	HS	
16	Inconel 713	Inconel 718	HS	Plate material sensitivity
17	Inconel 713	Inconel 718	HS	
18	Inconel 713	Inconel 718	HS	
19	TiAl	Steel	HS	Blade material sensitivity
20	TiAl	Steel	HS	
21	TiAl	Steel	HS	
22	TiAl	Inconel 718	HS	Speed sensitivity
23	TiAl	Inconel 718	HS	
24	TiAl	Inconel 718	HS	
25	FAIL			
26	Inconel 713 - Type 2	Inconel 718	HS	Blade geometry sensitivity
27	Inconel 713 - Type 2	Steel	HS	

Table 2: Blade Crush Test Matrix, Configuration 2.

SGs were installed in the pressure and suction side of the blades in configuration 1. 9 high speed cameras were used to record the impact sequence in the tests. After the tests, plates of configuration 2 were scanned in order to measure the maximum deformation of the plates.

5 LS-Dyna model description

Configuration 1 model consists of:

- Steel plate modelled with ***MAT_PLASTIC_KINEMATIC (MAT_003)** [5].
- Blade modelled with ***MAT_JOHNSON_COOK (MAT_015)** in the case of Inconel 713 blades (including failure) [5].
- Blade modelled with ***MAT_PIECEWISE_LINEAR_PLASTICITY (MAT_024)** in the case of TiAl blades. Failure based on principal stress and effective strain limits has been applied by including ***MAT_ADD_EROSION** [5].

See Annex for the material cards examples.

Initial speed has been applied to the steel plate. Free boundary conditions have been set in the blade.

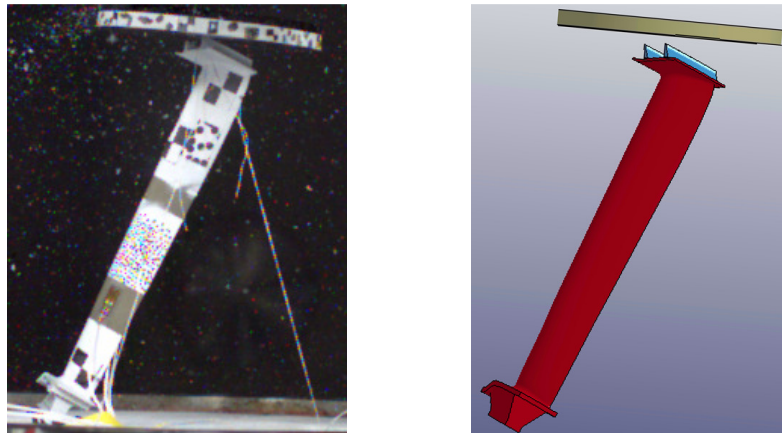


Fig.3: Test 6 positioning. Camera view (left) and model view (right)

Configuration 2 model consists of:

- Blade modelled with ***MAT_JOHNSON_COOK (MAT_015)** in the case of Inconel 713 blades (including failure).
- Blade modelled with ***MAT_PIECEWISE_LINEAR_PLASTICITY (MAT_024)** in the case of TiAl blades. Failure based on principal stress and effective strain limits has been applied by including ***MAT_ADD_EROSION**.
- Plate modelled with ***MAT_JOHNSON_COOK (MAT_015)** in the case of Inconel 718 plates (including failure).
- Plate modelled with ***MAT_PLASTIC_KINEMATIC (MAT_003)** in the case of steel plates. Failure based on triaxiality has been applied by including ***MAT_ADD_EROSION**.
- Support system modelled with ***MAT_PLASTIC_KINEMATIC (MAT_003)**.

See Annex for the material cards examples.

Initial speed has been applied to the blades. Fixed boundary conditions have been applied to the support system end.

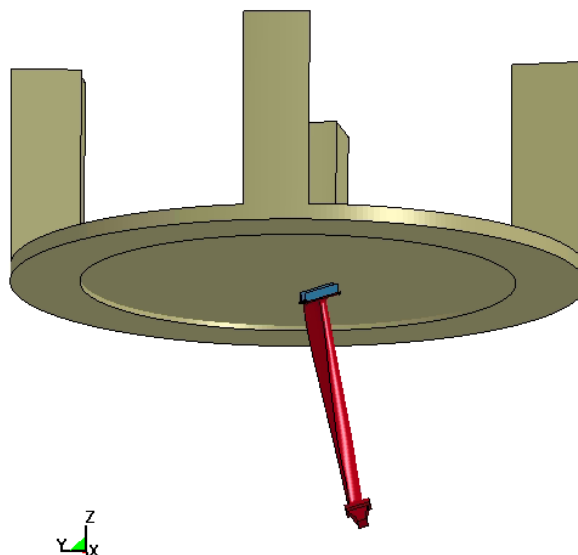


Fig.4: LS-Dyna set-up in the configuration 2- test 14 (Inconel 713 blade).

Sensitivity to the number of elements in the mesh of the plate has been performed in configuration 2. See figure below:

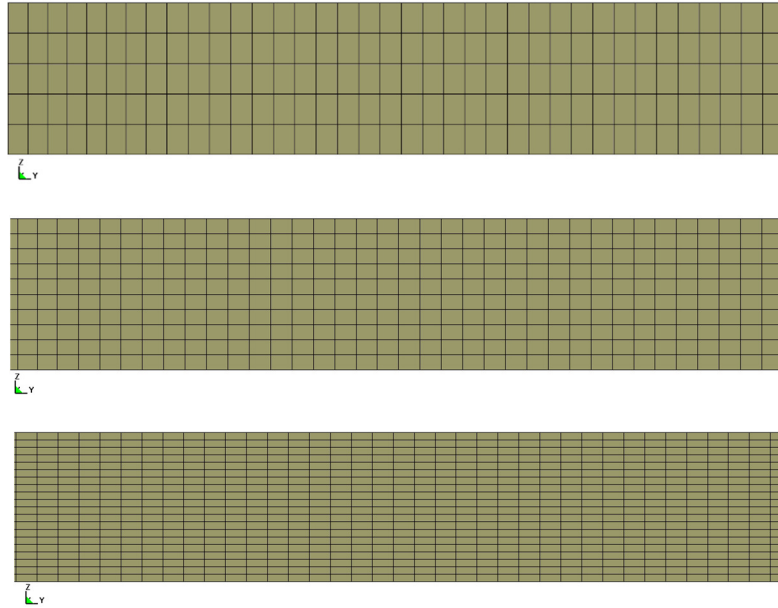


Fig.5: Configuration 2 steel plate mesh. 5 elements (up), 10 elements (middle) and 20 elements (down) in the thickness.

Contact in both configurations has been defined using: `*CONTACT_ERODING_SURFACE_TO_SURFACE`, including friction.

6 Test results and analysis correlation

The accuracy of the SG measurements has been checked with redundant data acquisition systems. The test results obtained are very consistent. Any difference between equivalent tests is due to small deviation of the projectiles, though there is no significant change in the impact behaviour.

6.1 Configuration 1

6.1.1 Inconel 713 blades

The impact sequence in Inconel 713 blades at high speed (HS) shows that the shroud of the blades is ejected at the beginning of the impact. Inconel 713 blade bends during the impact. LS-Dyna analysis impact sequence is in good agreement with high speed camera videos (see figures below).

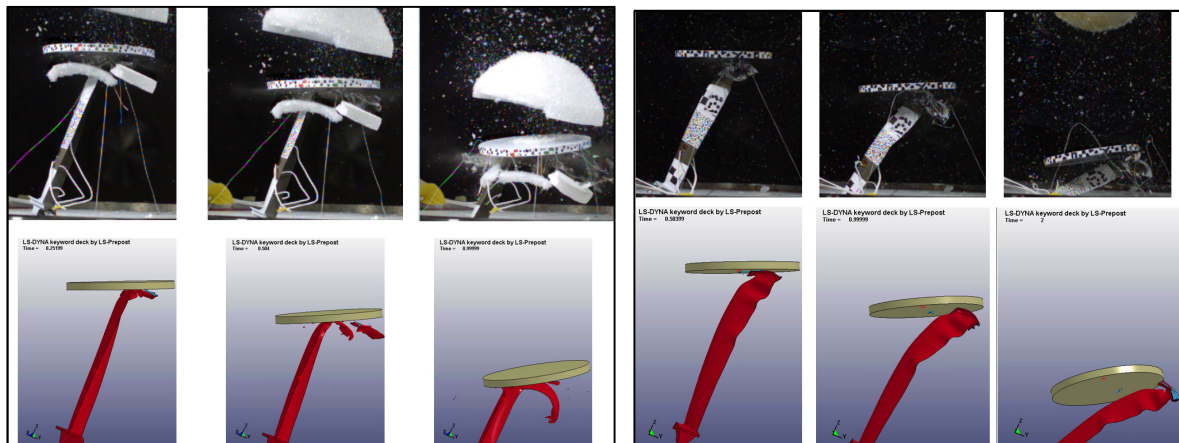


Fig.6: Inconel 713 blades impact sequence at HS (left) and LS (right) in configuration 1. Test results (up) and LS-Dyna analysis (down).

Initial compression and tensile waves are very well captured. See below (Figure 7) a comparison of SGs measurements and strain obtained in LS-Dyna:

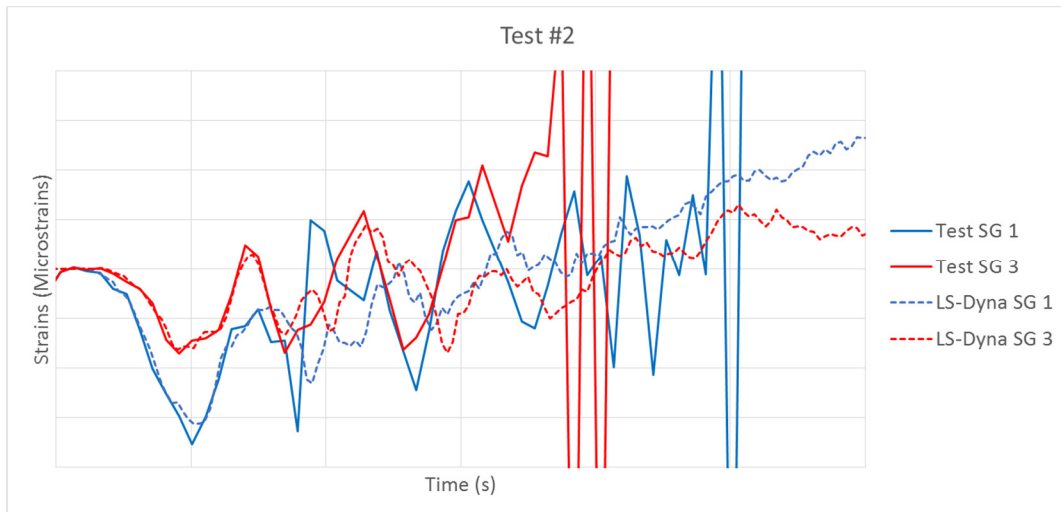


Fig.7: Test 2 SG results (solid line) and LS-Dyna analysis strains results (dotted line). SG #1 (blue) and SG #3 (red).

Final shape of the blade is also very similar between tests and LS-Dyna analyses (see Figure 8).

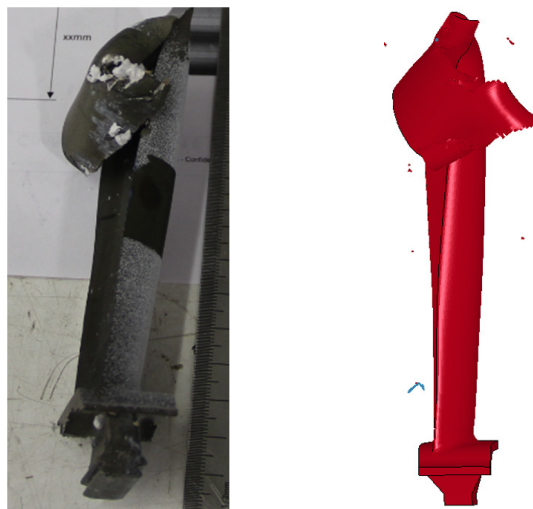


Fig.8: Inco713 blade damage after Test 4. Test (left) and analysis (right) results.

6.1.2 TiAl blades

The impact sequence in TiAl blades shows that there is no bending of the blade during the impact. TiAl blade starts cracking at the beginning of the impact and cracks propagate through the aerofoil. Similar results are obtained in HS and LS tests. LS-Dyna analysis impact sequence is in good agreement with high speed camera videos (see figures below).

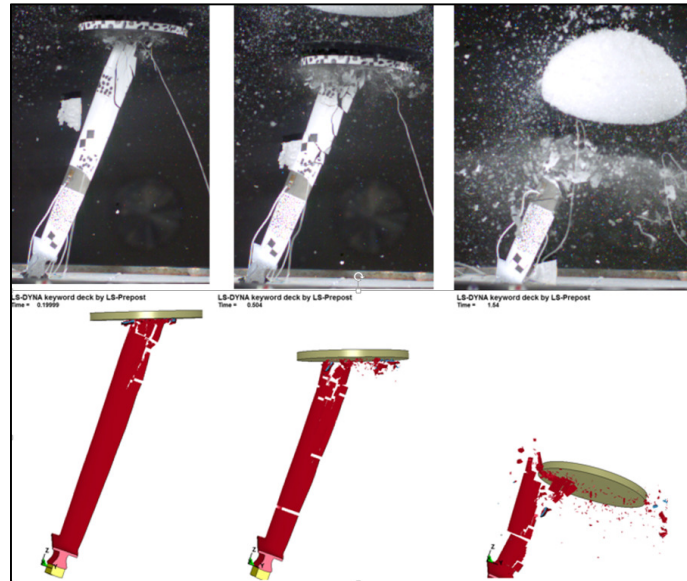


Fig.9: Test 8: TiAl blade impact sequence at high speed. Test (up), analysis (down).

The correlation of analysis and SG measurements shows very good results.

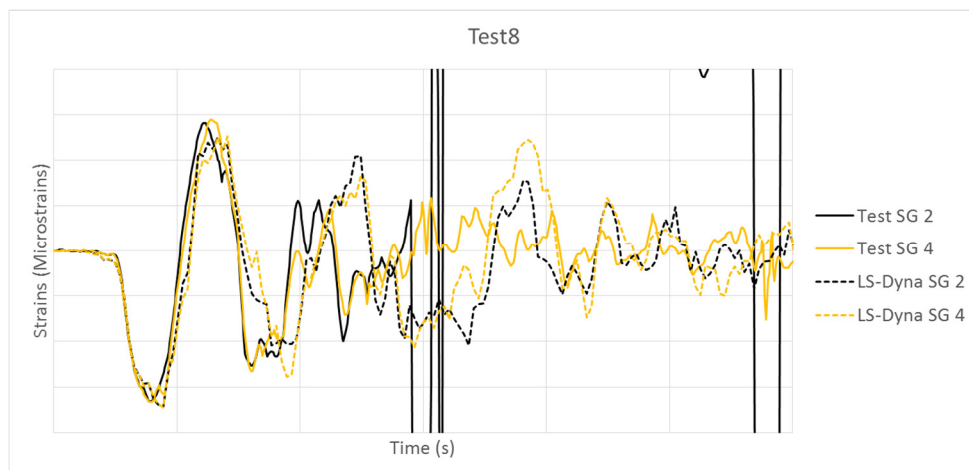


Fig.10: Test 8 SG results (solid line) and analysis strains results (dotted line). SG 2 (black, pressure side) and SG 4 (yellow, suction side).

6.2 Configuration 2

6.2.1 Inconel 713 blades

Test 18 is representative of configuration 2 impact with Inconel 713 blades and Inconel 718 plates. The following figure shows the comparison of the impact sequence between test and analysis:

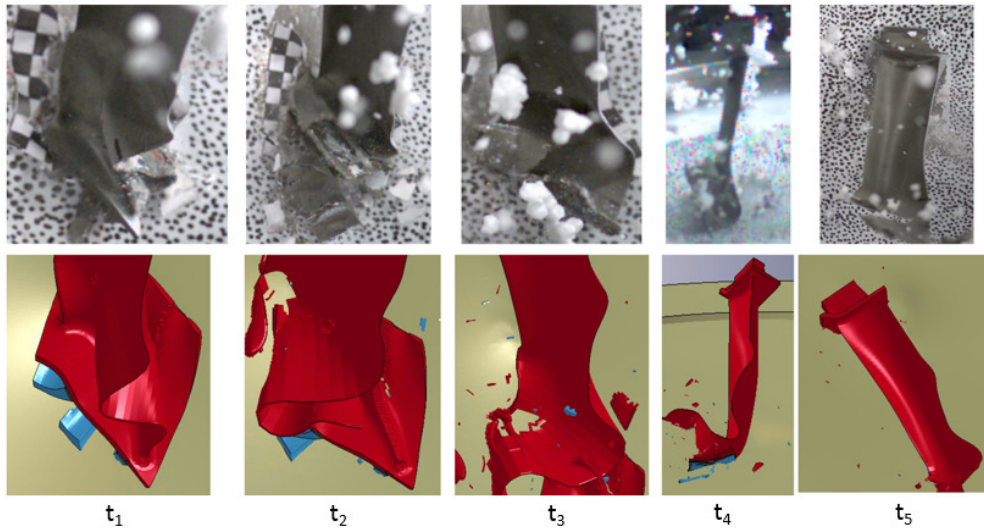


Fig.11: Test 18: Inconel 713 blade impact sequence. High speed camera (up), analysis (down), configuration 2.

The strain curves in the plate correlate well with the SG measurement. Note that the number of elements in the thickness of the plates affects the strain values in the surface of the plates. It is necessary to mesh the plate with at least 10 elements to match the strain measured in the SGs of the test. In the following figure it can be seen the better behaviour of the simulation measurements when the number of elements in the thickness is increased from 5 to 10 or 20 (see Figure 5 for plate mesh):

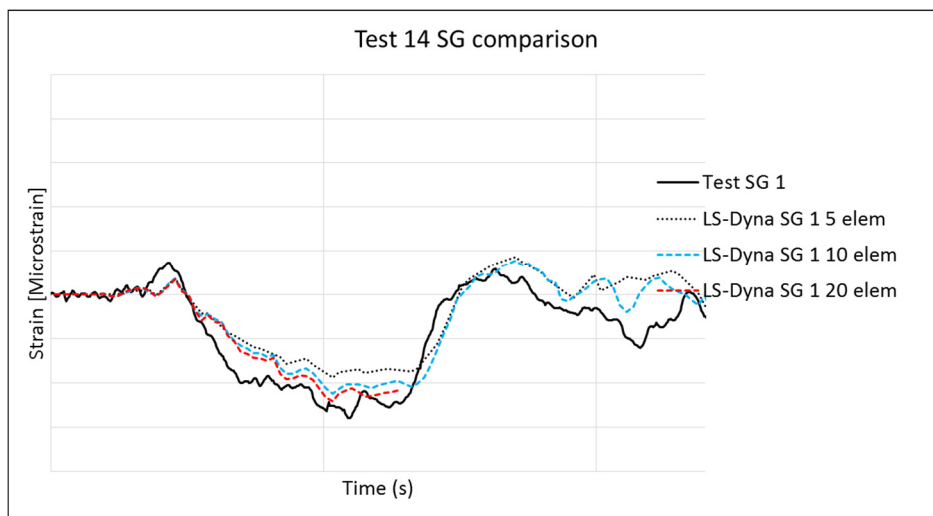


Fig.12: Test 14 steel plate SGs with 5 (black dotted line), 10 (blue dotted line) and 20 (red dotted line) elements in the thickness. Test 14 SG results (solid line) and analysis strains results (dotted lines).

There is good correlation between test and analysis. Blade shroud separates at the early stage of the impact (t_1). Blade bends and the root of the firtree hits again the plate. Figure below shows a comparison of the final shape of the blade and plates:

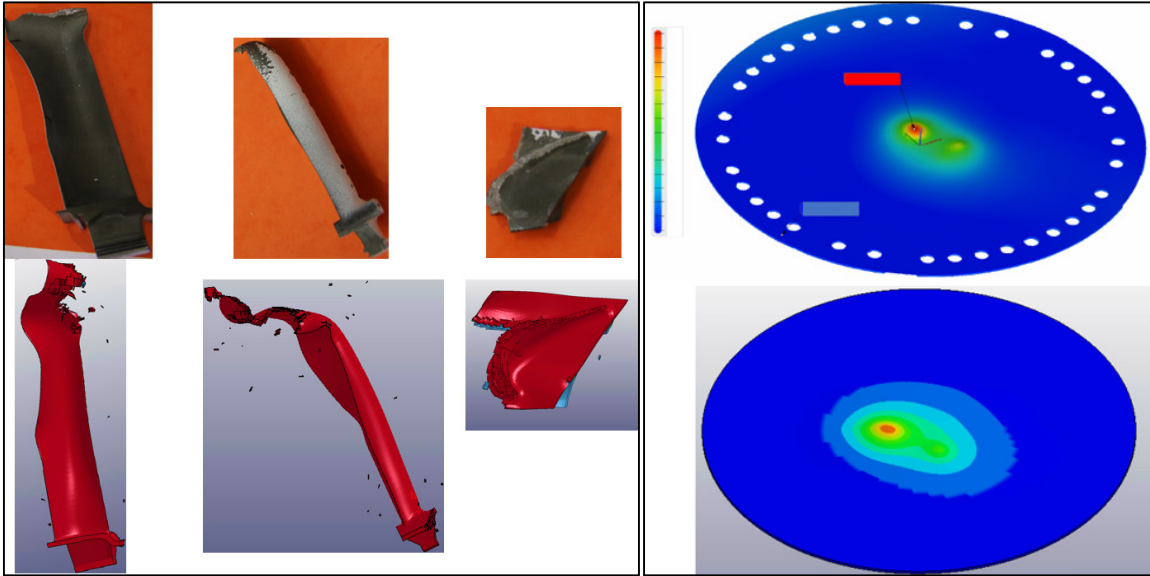


Fig.13: Final deformation of Inconel 713 blades (left) and plates (right). Test results (up) and analysis (down), configuration 2.

Similar results are obtained with the rest of Inconel 713 blades.

In general, the final shape of the Inconel 713 blades correlate well in configuration 2. The overall deformation of the Inconel 718 is also well captured.

6.2.2 TiAl blades

LS-Dyna analysis show good correlation with the impact sequence seen in TiAl configuration 2 tests. Blade does not bend during the impact and cracks propagates through the aerofoil. See figures below:

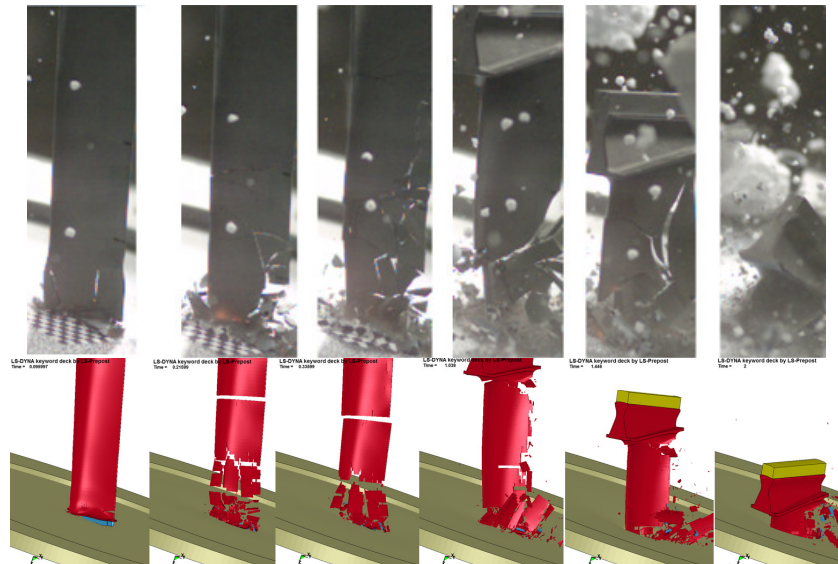


Fig.14: TiAl blade damage sequence in Test 20. Test (up) and analysis (down) results.

Final shape of the TiAl blades and Inconel 718 plates is similar to test results. There are small differences in the crack of the blades: Analyses show cracks at lower sections of the aerofoil than observed in the tests. Analyses predict well the crack shape in Inconel 718 plates (see Figure 15).

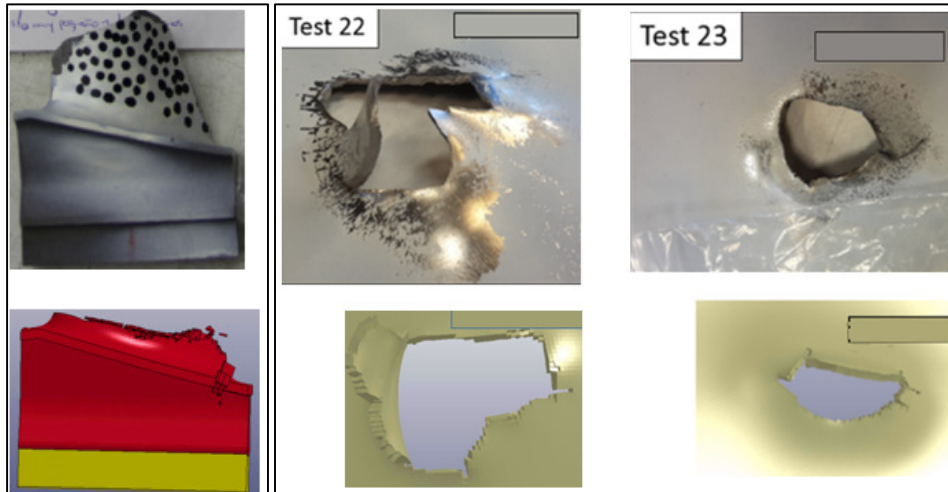


Fig.15: TiAl blade damage (left) and Inconel 718 plate damage (right) in configuration 2. Test (up) and analysis (down) results.

7 Summary

The work presented in this paper shows the capability of ITP Aero to perform impact rig tests that represent the initial containment impact conditions. This allows to test and compare the impact behaviour of different blade and casing materials in containment like conditions. The validation by analysis of these tests offers the possibility to study new containment conditions that will not require full turbine test campaigns or service experience.

The results and validation obtained in configuration 1 tests are representative of the initial impact sequence of the containment event. After the first impact, the Inconel 713 blade will bend and will interact with the trailing blades of the engine. In the case of TiAl blade, TiAl blade will break (not bending) and parts of the blade will hit the trailing blades.

The impact sequence of Inconel 713 blades and TiAl blades is quite different in configuration 2 tests. Inconel 713 blades bend and the impact is distributed along the sliding surface between blade and plate. On the contrary, many cracks appear in TiAl blades along the aerofoil when the tip hits the plate. There is no bending of the blade and, therefore, many sharp edges of the aerofoil hit the plate at the same impact position

LS-Dyna analyses show very good correlation of the impact sequence and the damage in Inconel 713 and TiAl blades in both configurations. The crack initiation in the plates correlate well with the analyses. This suggests that damage in a containment event would also correlate well even though the impact sequence is slightly different. The impact speeds validated in these tests and analyses are representative of engine impact conditions. Sensitivity to impact speeds shows good correlation, therefore, it is considered that the analysis would be applicable also at different speeds.

Future activities may include similar tests with additional turbine components and a full turbine containment rig test, in order to have a full validation of the containment event.

8 Acknowledgments

This project has received funding from the Clean Sky 2 Joint Undertaking in the European Union's Horizon 2020 research and innovation programme. The authors would like to express their gratitude to ITP Aero for supporting this research and permission to publish the paper.

9 Literature

- [1] European Union Aviation Safety Agency. "Certification Specifications and Acceptable Means of Compliance for Engines (CS-E)", Amendment 6, 24 June 2020, 190-191.
- [2] Cordasco, D., Emerling, W., Du Bois, P. "A Status Review of Failure Simulation at the Federal Aviation Administration". 11th European LS-Dyna Conference. 2017.
- [3] Dolci, S., Carney, K., Wang, L., Du Bois, P., Kan, C.D. "The effect of Inconel-718 High Strain Rate Sensitivity on Ballistic Impact Response using *MAT_224". 15th International LS-Dyna Users Conference. June 2018.
- [4] Memhard, D., Andrieux, F., Sun, D.Z., Häcker, R. "Development and verification of a material model for prediction of containment safety of exhaust turbochargers". 8th European LS-Dyna Users Conference, Strabough. May 2011.
- [5] Livermore Software Technology Corporation (LSTC), "LS-Dyna® Keyword User's Manual", LS-Dyna R11, 10 December 2018.

10 Annex

10.1 Material cards & Failure models

10.1.1 *MAT_PLASTIC_KINEMATIC (MAT_003) for Configuration 1 steel plates

```
*MAT_PLASTIC_KINEMATIC_TITLE
Confl_steel_plate_mat
$# mid ro e pr sigy etan beta
  &mat_003 &density &youngmod &poissrat &yields &etan 0.000
$# src srp fs vp
  0.000 0.000 0.000 0.000
```

10.1.2 *MAT_PLASTIC_KINEMATIC (MAT_003) for Configuration 2 steel plates (including failure)

```
*MAT_PLASTIC_KINEMATIC_TITLE
Conf2_steel_plate_mat
$# mid ro e pr sigy etan beta
  &mat_003 &density &youngmod &poissrat &yields &etan 0.0
$# src srp fs vp
  0.0 0.0 0.0 0.0
*MAT_ADD_EROSION_TITLE
erosion_steel
$# mid excl mxpres mneps effeps voleps numfip ncs
  &mat_003 0.0 0.0 0.0 0.0 0.0 1.0 1.0
$# mnpres sigpl sigvm mxeps epssh sigth impulse failtm
  0.0 0.0 0.0 0.0 0.0 0.0 0.0 0.0
$# idam dmgtyp lcsdg ecrit dmgepx dcrit fadexp lcregd
  1 1.0 &lcsdg &ecrit 1.0 0.0 0.0 0
$# sizflg refsiz nahsv lcsrs shrf biaxf lcdlim midfail
  0 0.0 0.0 0 0.0 0.0 0.0 0.0
$# lcfld epsthin engcrt radcrt
  0 0 0.0 0.0 0.0
```

10.1.3 *MAT_JOHNSON_COOK (MAT_015) for Inconel 713 (including failure)

```
*MAT_JOHNSON_COOK_TITLE
Inconel_713
$# mid ro g e pr dtf vp
  &mat_015 &density &shearmod &youngmod &poissrat 0.000 0.000
$# a b n c m tm tr epso
  &a_value &b_value &n_value &c_value &m_value &tm_value &tr_value &epso_val
$# cp pc spall it dl d2 d3 d4
  &cp_value 0.000 2.000000 0.000 &d1_value &d2_value &d3_value &d4_value
$# d5
  &d5_value
*EOS_LINEAR_POLYNOMIAL_TITLE
Inconel_713_EOS
$# eosid c0 c1 c2 c3 c4 c5 c6
  &mat_015 0.000 c1_value 0.000 0.000 0.000 0.000 0.000
$# e0 v0
  0.000 0.000
```

10.1.4 *MAT_JOHNSON_COOK (MAT_015) for Inconel 718 (including failure)

```

*MAT_JOHNSON_COOK_TITLE
Inconel_718
$# mid ro g e pr dtf vp
  &mat_015 &density &shearmod &youngmod &poissrat 0.000 0.000
$# a b n c m tm tr epso
  &a_value &b_value &n_value &c_value &m_value &tm_value &tr_value &eps_val
$# cp pc spall it dl d2 d3 d4
  &cp_value 0.000 2.000000 0.000 &dl_value &d2_value &d3_value &d4_value
$# d5
  &d5_value
*EOS_LINEAR_POLYNOMIAL_TITLE
Inconel_718_EOS
$# eosid c0 c1 c2 c3 c4 c5 c6
  &mat_015 0.000 c1_value 0.000 0.000 0.000 0.000 0.000
$# e0 v0
  0.000 0.000
    
```

10.1.5 *MAT_PIECEWISE_LINEAR_PLASTICITY (MAT_024) for TiAl (including failure)

```

*MAT_PIECEWISE_LINEAR_PLASTICITY_TITLE
TiAl
$# mid ro e pr sigy etan fail tdel
  &mat_024 &density &youngmod &poissrat &yields 0.0001.0000E+21 0.000
$# c p lcsc lcsr vp
  0.000 0.000 &lcsc &lcsr 0.000
$# eps1 eps2 eps3 eps4 eps5 eps6 eps7 eps8
  0.000 0.000 0.000 0.000 0.000 0.000 0.000 0.000
$# es1 es2 es3 es4 es5 es6 es7 es8
  0.000 0.000 0.000 0.000 0.000 0.000 0.000 0.000
*MAT_ADD_EROSION_TITLE
erosion_TiAl_Principal_Stress
$# mid excl mxpres mneps effeps voleps numfip ncs
  &mat_024 0.0 0.0 0.0 &fstrain 0.0 1.000000 2.000000
$# mnpres sigpl sigvm mxeps epssh sigth impulse failtm
  0.0 &fstress 0.0 0.0 0.0 0.0 0.0 0.0
$# idam dmgtyp lcsdg ecrit dmgepx dcrit fadexp lcregd
  1 1.0 &lcsdg &ecrit 1.0 0.0 0.0 0
$# sizflg refsiz nahsv lcsrs shrf biaxf lcdlim midfail
  0 0.0 0.0 0 0.0 0.0 0.0 0.0
$# lcfld epsthin engcrt radcrt
  0 0 0.0 0.0 0.0
*DEFINE_CURVE_TITLE
Triaxiality_Strain_curve_TiAl
$# lcid sidr sfa sfo offa offo dattyp
  &lcsc 0 1.000000 1.000000 0.000 0.000 0
$# al ol
    
```